

NOVEL GRAPHICAL DESIGN METHOD FOR HYBRID PROCESSES

Mark Peters, Shehzaad Kauchali, Diane Hildebrandt, and David Glasser
Centre of Material and Process Synthesis, School of Chemical and Metallurgical Engineering
University of the Witwatersrand, Private Bag 3, WITS 2050, Johannesburg, South Africa
mark.peters2@wits.ac.za, shehzaad.kauchali@wits.ac.za, diane.hildebrandt@wits.ac.za,
david.glasser@wits.ac.za

Abstract

Shortcut methods for the design and synthesis of separation systems are useful, especially in the conceptual stages of a process design. However, current approaches incorporated in these techniques result in them being suitable for traditional designs only, and unable to manage novel or complex configurations. Using column profile trajectories to describe the compositional behaviour of material in both distillation and membrane sections, it will be shown how any configuration, no matter how complex, can be modelled. With this comes an overall deeper understanding of the operation of the chosen system. As an example, a Petlyuk-type arrangement will be considered – firstly incorporating membrane permeation units as the only means of separation, and then secondly linking membrane units with distillation thereby forming a hybrid. The feasibility of each design is discussed, and compositional regions of feasibility are established, where necessary. Although the nature of column profiles may appear to be complicated, this method allows one to quickly and easily understand complex configurations, thus saving time, money and potentially reducing energy consumption.

Keywords: Hybrid distillation-membrane, Graphical, Design, Column Profiles.

1. Introduction

Distillation is the most commonly used method for separation of fluid mixtures. Several advances have been made to formulate shortcut methods of design^{1,2}, with complex column configurations emerging in an attempt to reduce equipment sizes. While the Petlyuk column is the most popular of these advances, other variations exist. Theoretically, these column configurations have the ability to produce the required products, but their operation is complex, thus resulting in a lack of reliable design methods. In some instances, it becomes difficult or even impossible to separate some mixtures by distillation alone. Hybrid arrangements provide an alternative solution to this. Various shortcut methods of design have been proposed for hybrid distillation-membrane processes^{3,4}. However, most of these are either only suitable for a single configuration, thereby limiting the design procedure, or they provide little insight into the location of feed and side-draw streams, as well as number of stages or membrane area needed. Thus, a more creative design approach needs to be employed.

Graphical methods of design have shown their value in several separation systems. Tools such as Distillation Residue Curve Maps (D-RCM's), operation leaves¹ and, Column Profile Maps (CPM's)⁵ emerged so as to assist design engineers in analysing such systems. Holland et al.⁶ used the "moving triangle" phenomenon in CPMs to design complex distillation configurations. Membrane Residue Curve Maps (M-RCM's) were proposed by Peters et al.⁷, with the intention of formulating a similar graphical technique for membrane systems. This then allows one to evaluate both membrane permeation and distillation from the same viewpoint. Column Sections (CS), initially identified by Tapp et al.⁵ for distillation systems, were adapted for membrane processes.

In this paper, the ideas and phenomena related to column profiles are used to both mathematically and graphically analyse hybrid distillation-membrane configurations. As an illustration, a Petlyuk-type arrangement will be considered. Some simplifying assumptions and operating conditions are made, allowing one to evaluate the feasibility of such arrangements. It is not the aim of this article to completely solve complex membrane and hybrid arrangements, but rather to introduce the idea as to how column profiles can be used to understand and design such processes.

2. Column Sections

A CS is defined as a length of column between points of addition and removal of material and/or energy⁵. This statement is general and can be applied to not only distillation, but membranes too. Figure 1 graphically shows CSs for distillation and membrane. Table 1 details the nomenclature used.

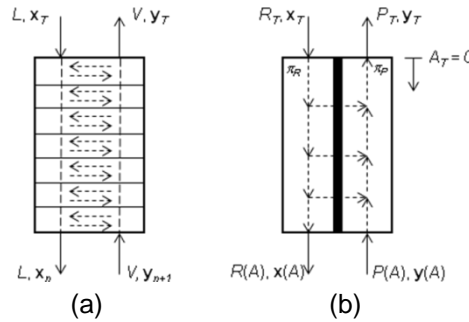


Figure 1. Generalized column sections (CS). (a) Distillation, (b) Membrane.

The assumption of *constant molar overflow* is often justified in distillation CSs. Operation in membrane CS is different: permeation is mono-directional, and will occur from retentate to permeate, but not in the reverse direction, resulting in a continual change in the flows within in any membrane CS. As drawn in Figure 1(b), both the retentate and permeate will have their maximum values at the top of the CS (namely, R_T and P_T). The compositional change of material down the length of any CS is described by the Difference Point Equation (DPE). For the distillation and membrane sections, the change in the liquid or retentate composition (\mathbf{x}) with respect to position (n or A) can be described by equations 1 and 2, respectively. Table 1 details the nomenclature that applies.

$$\frac{d\mathbf{x}}{dn} = \left[\frac{1}{r_{\Delta D}} + 1 \right] [\mathbf{x} - \mathbf{y}(\mathbf{x})] + \frac{1}{r_{\Delta D}} [\mathbf{X}_{\Delta D} - \mathbf{x}] \quad (1)$$

$$\frac{d\mathbf{x}}{dA} = \left[\frac{1}{r_{\Delta M}} + 1 \right] [\mathbf{x} - \mathbf{y}(\mathbf{x})] + \frac{1}{r_{\Delta M}} [\mathbf{X}_{\Delta M} - \mathbf{x}] \quad (2)$$

Table 1. Nomenclature and symbols used in Figures 1(a) and (b), and equations 1 and 2.

	Distillation	Membrane
Subscript or Superscript	D	M
Column Section reference	DCS	MCS
Downward material flow and composition	Liquid L, \mathbf{x}	Retentate $R(A), \mathbf{x}$
Upward material flow and composition	Vapour V, \mathbf{y}	Permeate $P(A), \mathbf{y}$
Position Variable	Stages n	Area A
Net flow	$\Delta_D = V - L$	$\Delta_M = P(A) - R(A)$
Difference Point	$\mathbf{X}_{\Delta D} = \frac{V\mathbf{y} - L\mathbf{x}}{\Delta_D}$	$\mathbf{X}_{\Delta M} = \frac{P(A)\mathbf{y} - R(A)\mathbf{x}}{\Delta_M}$
Reflux Ratio	$r_{\Delta D} = \frac{L}{\Delta_D}$	$r_{\Delta M} = \frac{R(A)}{\Delta_M}$

A subscript of “T” will be used to refer to quantities at the Top of a CS

Although the DPEs for each section (equations 1 and 2) share the same mathematical form, there are some subtle, yet important differences: (i) Each DPE is describing a unique system, and the way in which $\mathbf{y}(\mathbf{x})$ is modelled relates to the operation of each process. (ii) The flows of the liquid and vapour streams in the DCS are constant, resulting in fixed values for Δ_D , $\mathbf{X}_{\Delta D}$, and $r_{\Delta D}$. (iii) In the MCS, the flows of the retentate and permeate are decreasing in value from the top of MCS down, but it can be shown by material balance that Δ_M and $\mathbf{X}_{\Delta M}$ are constant. However, $r_{\Delta M}$ varies in magnitude, also having its maximum value at the top of the MCS. This has to be accounted for in equation 2, resulting in the scalar terms changing with position (A). This causes significant differences in the behaviour of the column profiles for MCS when compared to that of DCS.

For demonstration purposes, simple vapour-liquid equilibrium (VLE) and permeation flux models will be used to mathematically describe the vapour and permeate compositions, respectively. A constant relative volatility VLE model is used for distillation, as described in equation 3, while a constant relative permeability flux model for gas separation is used for membrane sections, as given in equation 4.

$$\text{VLE: } y_i = \frac{\alpha_{ij}^D x_i}{\sum_i \alpha_{ij}^D x_i} \text{ and, Permeation: } y_i = \frac{\alpha_{ij}^M x_i}{\sum_i \alpha_{ij}^M x_i} \quad (3,4)$$

where α_{ij}^D is the relative volatility, while α_{ij}^M is the relative permeability. The form of equations 3 and 4 may be the same, but this occurs because vacuum conditions are being maintained on the permeate side in the MCS. One can show that for MCS, the retentate flow can be modelled using:

$$\frac{dR(A)}{dA'} = -\sum_i \alpha_{ij}^M x_i \quad \text{where } A' = A \frac{\pi_R P_{ref}}{\delta} \text{ is a scaled dimensionless area.} \quad (5)$$

The retentate flow is a function of position as well as its corresponding composition. The DPEs (equations 1 or 2), in conjunction with the corresponding equilibrium or flux models (equation 3, or 4 and 5, respectively) allows one to graphically interpret the compositional change of \mathbf{x} down the length of each of the CS. Profiles for \mathbf{y} can also be generated by material balance (refer to Table 1).

3. Hybrid Distillation-Membrane Design

As a case study, a membrane module thermally-linked to a distillation column will be analysed, such as the Petlyuk-type arrangement shown in Figure 2(a). Distillation is equilibrium-based, while membrane permeation is rate-based, and combining the two into a hybrid should allow for each one to operate in the compositional space where it is best-suited. Since no specifications about the number of stages, membrane area, or feed/side-draw locations have been made, the arrangement can be considered to be a super-structure. There are a number of possible variations to the configuration, not shown here, but analysing the hybrid design proposed in Figure 2(a) does not limit one to a set design, but rather encompasses a wide range of configuration options. Of course, in conceptual design stages, it is required to discern whether an arrangement of equipment is feasible or not.

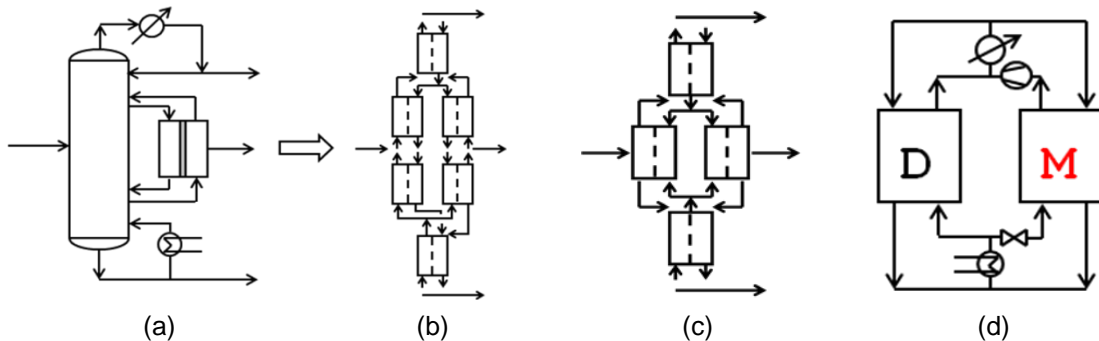


Figure 2. (a) Petlyuk-type arrangement for membranes. (b) Column Section breakdown. (c) Petlyuk arrangement operating at overall infinite reflux. (d) Coupled distillation and membrane CSs.

Any configuration can be broken down into a number of CSs, no matter how complex in its design. The CSs are simply identified between the points of addition and removal of material. The CS breakdown for the hybrid Petlyuk is shown in Figure 2(b). Now, it is assumed that the *overall* arrangement is operating at infinite reflux, implying that the addition of feed, or removal of product will have negligible effects on the overall on the flows within each CS. There will still, however, be comparable differences in the flows within each CS. The process in Figure 2(b) is then simplified as displayed in Figure 2(c). Because any material entering the top CS in Figure 2(c) must also leave at the same point, this section is performing the same operation as the condenser mixing material from the middle two sections, and then returning it to these sections at different compositions. Likewise about the bottom section behaving like a reboiler. This then allows further simplification, as given in Figure 2(d).

Although the top and bottom sections are not present in the simplified diagram (Figure 2(d)), they do in fact exist. Under the assumption of infinite reflux, the DPE for these two sections in Figure 2(c) reduces to the membrane residue curve equation⁷. This implies that their respective profiles will follow *residue curves*. Verifying the feasibility of this simplified form of a hybrid combination, as shown in Figure 2(d), would give insight and answers about the operation and possibilities of the entire design.

Material Balances: In Figure 2(d), the same nomenclature is associated with each CS as given in Figures 1(a) and (b). The following material balance relationships result:

$$\Delta_M = -\Delta_D, \text{ and } r_{\Delta M}|_T = -r_{\Delta D}, \text{ and } \mathbf{X}_{\Delta M} = \mathbf{X}_{\Delta D} = \mathbf{X}_\Delta \quad (6-8)$$

The reflux ratio in the MCS decreases down its length, while the reflux ratio in the DCS remains constant. Thus, the designer has the freedom of choosing the reflux ratio and difference point for one CS. The same quantities for the other CS are set by mass balance. The following operating conditions will be assumed: $r_{\Delta M}|_T = 5 = -r_{\Delta D}$, $\mathbf{X}_{\Delta M} = [0.3, 0.3] = \mathbf{X}_{\Delta D}$, $\alpha_{AB}^D = 3$, $\alpha_{BB}^D = 1$ and $\alpha_{CB}^D = 1.5$, $\alpha_{AB}^M = 3$, $\alpha_{BB}^M = 1.5$ and $\alpha_{CB}^M = 1$. The respective α -values used for distillation and membrane permeation are different – it is assumed that one would use a membrane that has different separation capabilities to that of the distillation. Note that $r_{\Delta M} > 0$, while $r_{\Delta D} < 0$.

Requirements for Feasibility: For a feasible coupled column section arrangement, it is required that the retentate profile intersects with the liquid profile, as well as the permeate profile intersecting with the vapour profile. Also, the direction of movement of the profiles, and the order of intersection must be in accordance with the flow arrangement in the coupled CS configuration, (see Figure 2(d)). It is already known that the liquid and retentate profiles will always intersect (at \mathbf{x}_T). Thus, all possible intersections between the vapour and permeate profiles need to be sought for a feasible arrangement.

Permeate Profiles: Irrespective of the location of its starting point of any general membrane permeate profile, it can be shown that its termination point is fixed at \mathbf{X}_Δ , and occurs as $r_{\Delta M} \rightarrow 0$ (this can be determined from the DPE in equation 2). This can be confirmed by the arbitrarily plotted profiles in Figure 3. No matter the location of \mathbf{x}_T , both the retentate and permeate profiles will move in a direction so as to seek their respective “mobile” stable nodes as $r_{\Delta M} \rightarrow 0$. At some point, both profiles would very closely follow their stable node pinch point loci. This is demonstrated in Figure 3 for the permeate pinch point loci. (Note that the permeate pinch point locus differs from that of the retentate by material balance, and is calculated accordingly.) Since it is assumed that $r_{\Delta M} > 0$, the location and movement of the *positive branch* of the permeate stable node pinch point locus is of interest.

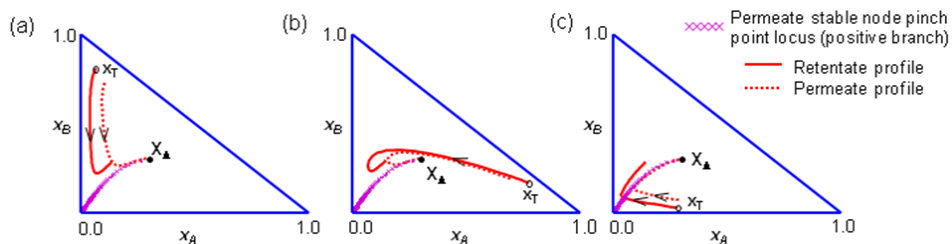


Figure 3. (a) – (c) Commencing the retentate profiles at various \mathbf{x}_T -values. The corresponding permeate profile eventually always approximates its pinch point curve.

Remembering that it is required to find where the vapour profile intersects with the permeate profile, one can now rather search for the vapour profiles that intersect with the permeate pinch point locus. This is valid since all permeate profiles eventually follow the pinch point locus. It may be argued that the actual permeate profile only follows the pinch point locus for a short while. However, as one varies the magnitude of R_T (and hence P_T) the profile follows the pinch point locus for longer. Also, as will be revealed later, the location of \mathbf{x}_T 's that results in feasibility, as well as the relative position of the vapour and permeate to each other, is such that an intersection with the permeate pinch point locus is guaranteed. While it is agreed that the permeate profile does not match the pinch point locus exactly, it is very close proximity to the locus. Thus, using the pinch point locus is justified, especially for conceptual stages of synthesis and design, where accuracy is not of great importance.

The location of \mathbf{y} relative to \mathbf{x} : For both the DCS and MCS, the respective vapour and permeate curves are determined by mass balance. For the MCS, $r_{\Delta M} > 0$, implying that each \mathbf{y} has to lie between \mathbf{X}_{Δ} and the corresponding \mathbf{x} co-ordinate. For the DCS, $r_{\Delta D} < 0$ signifies that \mathbf{x} now lies between \mathbf{X}_{Δ} and \mathbf{y} , on the straight line that connects them. Thus, the position of the permeate profile with respect to the retentate is on the opposite side of the vapour profile compared to the liquid.

Vapour Profiles: It needs to be established what region of \mathbf{x}_T , within the MBT, yields feasibility. Consider 2 arbitrarily chosen starting conditions for the liquid profiles, as shown in Figure 4. Their corresponding vapour profiles are plotted as well. In Figure 4, in one case the vapour profile lies below the liquid profile, while in another it lies above. This arises since the position of the vapour curve relative to its liquid curve is determined by \mathbf{X}_{Δ} . Out of the two profiles shown, only the one with the vapour positioned below the liquid is useful since it would pass through the permeate stable node pinch point locus. This is not the only profile that would exhibit such an intersection, but rather there are numerous profiles that would satisfy this condition. Since their dependency on \mathbf{X}_{Δ} is significant, all these profiles would exist in a defined region. This region would have to exist within the MBT. The relevant vapour curves are required to pass through the permeate stable node pinch point locus, so they would have to commence at a point before the locus, so their direction of movement ensures an intersection with the locus. In this case, all profiles to the right of the locus move in the appropriate direction. Thus, the permeate stable node pinch point locus forms a boundary of the feasible region.

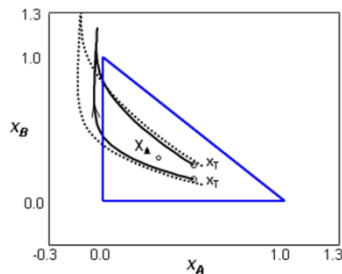


Figure 4. Some liquid profiles (solid), and their corresponding vapour profiles (dashed) relative to \mathbf{X}_{Δ} .

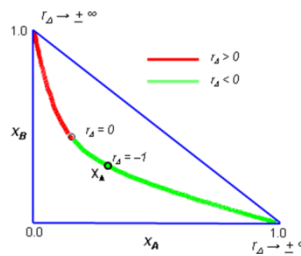


Figure 5. Liquid pinch point locus within the MBT.

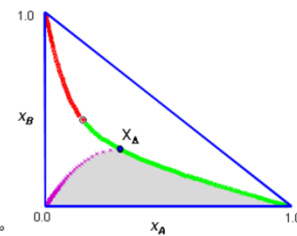


Figure 6. The permeate (purple) and liquid (green) pinch point loci defining an initial region of feasibility.

Liquid Pinch Point Locus: It is evident from Figure 4 that the relative position of the vapour changes from below to above the liquid profile as \mathbf{x}_T is altered. This means that at some starting point between these two extremes, the vapour curve, although commencing behind the liquid, would appear to follow the same trajectory as the liquid. It is worth noting that this overlap between the profiles would only occur up until some point when the two curves would diverge from each other, heading off to their respective pinch points. Now, in order to obtain this overlap between the profiles, the initial \mathbf{y} -value not only must lie on the straight line connecting \mathbf{X}_{Δ} and \mathbf{x} produced, but the line should also be tangent at \mathbf{x} . This coincides with the definition of a pinch point for the liquid – by equating the DPE to zero: $(1 + r_{\Delta D})(\mathbf{x} - \mathbf{y}(\mathbf{x})) = -(\mathbf{X}_{\Delta} - \mathbf{x})$. This is saying that the points \mathbf{x} , \mathbf{y} and \mathbf{X}_{Δ} are collinear, and the straight line connecting them is tangent to the profile commencing at \mathbf{x} . If a point on the liquid pinch point curve is used as \mathbf{x}_T , then the two profiles would overlap. This would be the case for all points on the liquid pinch point locus. Thus, the liquid pinch point locus forms another boundary of the feasible region! For the α^D -values assumed, and the \mathbf{X}_{Δ} -value chosen, the liquid pinch point curve is plotted in Figure 5. Only the part of the curve within the MBT is shown, since this is the only section that is of importance. Superimposing the permeate stable node pinch point curve on Figure 5, and remembering that all \mathbf{x}_T -values to the right of it allow for a feasible intersection, the region can be initially defined, as shown in Figure 6. Both the pinch point loci pass through and share the same \mathbf{X}_{Δ} . The only part of the liquid pinch point locus that is now relevant to the situation is the negative branch of the unstable node. This is expected since $r_{\Delta D} < 0$, and the profiles are required to move away from the unstable node towards the stable, intersecting with the permeate pinch point locus on the way.

Shifted Distillation Triangle: All the liquid profiles for the DCS exist on a single map known as a Column Profile Map (CPM)⁵, defined as a linear transform of the Residue Curve Map (RCM). i.e. the profiles in the RCM have, graphically speaking, been shifted and rotated slightly in order to produce the CPM. In doing so, the three nodes move as well from the pure component locations. Holland et

al.⁸ discuss the direction of the eigenvectors at each of the shifted nodes is such that one can connect the nodes with straight lines, thus forming a triangle, known as “moved” triangle, from the original MBT. The CPM using the assumed values chosen for the DCS discussed above is plotted in Figure 7. The permeate profiles will always move towards \mathbf{X}_Δ and terminate there. It should be obvious that only liquid (and hence vapour) profiles within the shifted triangle will result in a feasible arrangement. This is due to their direction of movement. The feasible region obtained in Figure 6 is further reduced in spatial size, as shown in Figure 8. This region shows all possible \mathbf{x}_T -values that will result in the coupled distillation and membrane sections being feasible, for the operating conditions assumed.

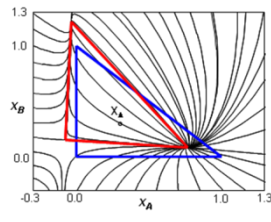


Figure 7. CPM for the DCS at $r_{AD} = -5$ and $\mathbf{X}_\Delta = [0.3, 0.3]$. MBT in blue, shifted triangle in red.

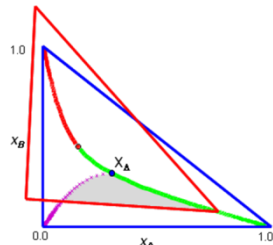


Figure 8. Region of possible \mathbf{x}_T locations, for the operating conditions chosen, that would result in a feasible arrangement.

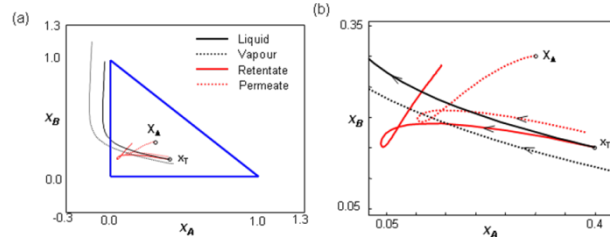


Figure 9. (a) Column profiles for the membrane and distillation sections with \mathbf{x}_T in the feasible region. (b) Zoomed in version of (a).

Column Profiles: Figure 9(a) shows the profiles obtained for an arbitrarily chosen \mathbf{x}_T within the region. Figure 9(b) is a zoomed version of Figure 9(a). It can be seen that the vapour and permeate profiles intersect twice. This indicates that multiple steady states in hybrid processes is very possible and needs to be taken into account, especially for control purposes. Starting at any point outside this region would result in an infeasible configuration. As with the coupled membrane scenario, to complete the design, one would generate the residue curves for the top and bottom sections (Figure 2(c)) commencing at the appropriate compositions, and terminating at the pure components.

Regions of Feasibility: General: Although this region was generated for a specific set of operating conditions, the theory can be extended to any chosen values of \mathbf{X}_Δ , α_D , α_M , and r_{AD} (or r_{AM}). No matter what the conditions are, the region, if it exists, can be found by enclosing the area formed between (i) the positive branch of the pinch point locus for stable node of the *permeate*, (ii) the negative branch of the pinch point locus for the unstable node of the *liquid*, and (iii) the region within the moved triangle. Of course, the region has to lie within the bounds of MBT.

4. Conclusion

Although the method shown in this chapter is useful for conceptual stages of a design, it does provide a very good initialization point in rigorous simulation packages when more accurate and detailed results are needed. Because there is a deeper understanding of the operation of the system, the designer is able to make insightful decisions early on, hence saving money and time. It should be appreciated that this work is not applicable to membrane permeation and distillation only, but can easily be adapted for *any* separation method. With both constant and non-constant flow assumptions have been tackled here, this then equips one to use the methods displayed for the separation procedure of their choice. Of course, details of equilibrium/flux model, flow assumptions and directions, etc. need to be decided upon. But the method and results arrived at here would still apply.

References

1. Castillo, F. J. L. et al., *Ind. Eng. Chem. Res.*, **1998**, 37, 987–997.
2. Fien, G. A. F. and Liu, Y. A., *Ind. Eng. Chem. Res.* **1994**, 33, 2505–2522.
3. Bausa, J. and Marquardt, W., *Ind. Eng. Chem. Res.* **2000**, 39, 1658–1672.
4. Huang, Y. et al., *Chem. Eng. Sci.* **2004**, 59, 2863–2879.
5. Tapp, M. et al., *Ind. Eng. Chem. Res.*, **2004**, 43, 364–374.
6. Holland, S. et al., *Comput. Chem. Eng.* **2004**, 29, 181–189.
7. Peters, M. et al., *Ind. Eng. Chem. Res.*, **2006**, 45, 9080–9087.
8. Holland, S. et al., *Ind. Eng. Chem. Res.*, **2004**, 43, 3590–3603.